6. Post-reaction Characterization

In the aim to explore the surface after reaction, the reacted HOPG samples were investigated with different techniques including Scanning Electron Microscopy (SEM), Atomic Force Microscopy (AFM) and Temperature Programmed Spectroscopy techniques including Thermal Programmed Desorption (TPD), Thermal Programmed Oxidation (TPO) and Thermal Programmed Desorption in CO atmosphere (TP(CO)).

6.1 Post reaction thermal programmed analysis

In figure 6.1, the TPD spectra of a cleaved annealed HOPG sample are shown. No desorption peaks of water, hydrogen or carbon oxides can be detected for such a clean thermally stable surface. The background starts to increase at about 450 ^{o}C with extreme rise above 800 ^{o}C. This is a result of desorption from the sample holder and other UHV components which increases the pressure in the whole UHV chamber and consequently, the background.

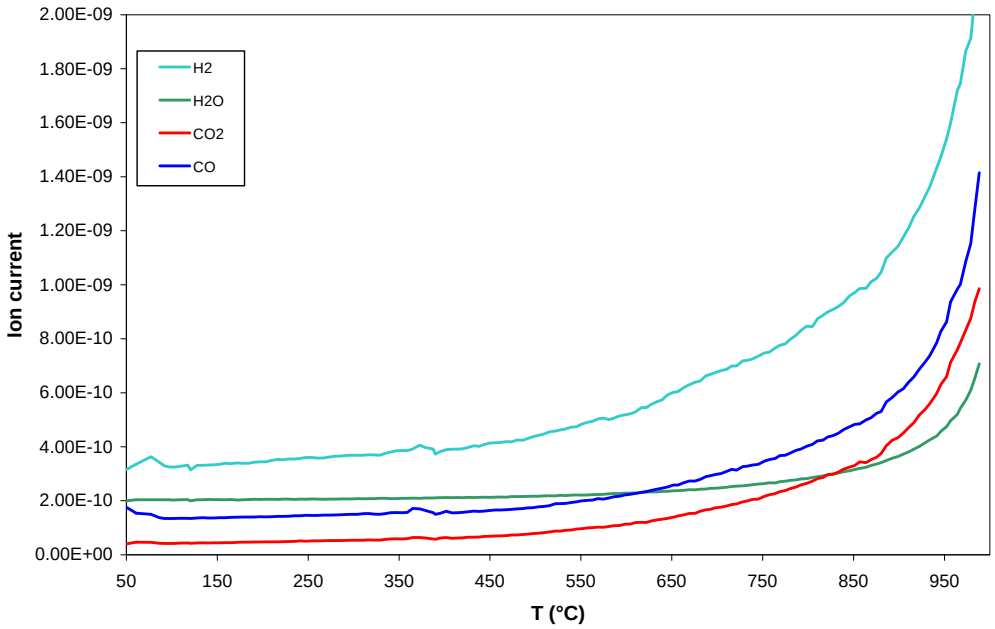

Figure 6.1 TPD of HOPG before reaction

In the TPD experiment for an HOPG sample after oxidative dehydrogenation reaction of ethylbenzene, only carbon monoxide and carbon dioxide desorption peaks were observed (Figures 6.2). This suggests that the surface is covered by deposits

composed mainly of carbon and oxygen. The absence of hydrogen or water desorption peaks indicates the absence of any hydrocarbons or hydrogen-containing groups in the depositions over the catalyst surface.

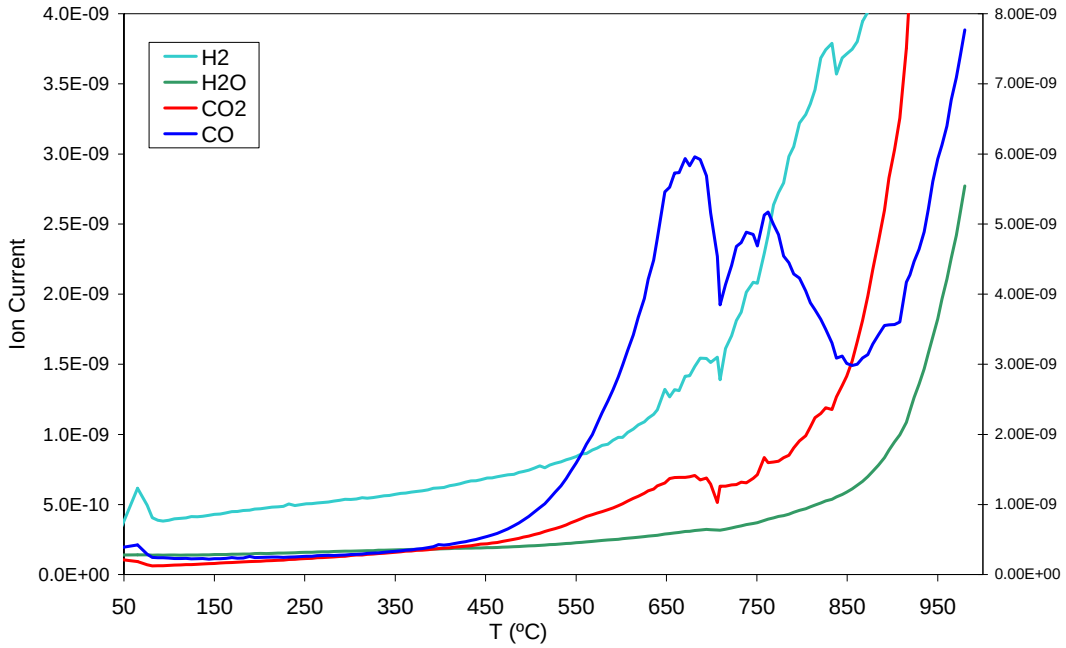

Figure 6.2 TPD spectra of cleaved HOPG after ODH reaction (20 ml/min, 0.5% EB, 1% O_2, 120 min, 400 ^oC) *(Right y axes corresponds to CO signal)*

Upon applying TPO investigation, ($P(O_2)$: $1x10^{-7}$ mbar) carbon monoxide and carbon dioxide desorption peaks were also observed from the reacted sample (figure 6.4), TPO spectra of a cleaved sample is given in figure 6.3 for comparison. These peaks appeared at the same desorption temperatures observed in TPD experiment.

Exactly as expected from the TPD experiments, no desorption peak of water was observed. This experiment proves again what was found in the previous experiment about the carbon deposits being composed of carbon and oxygen only.

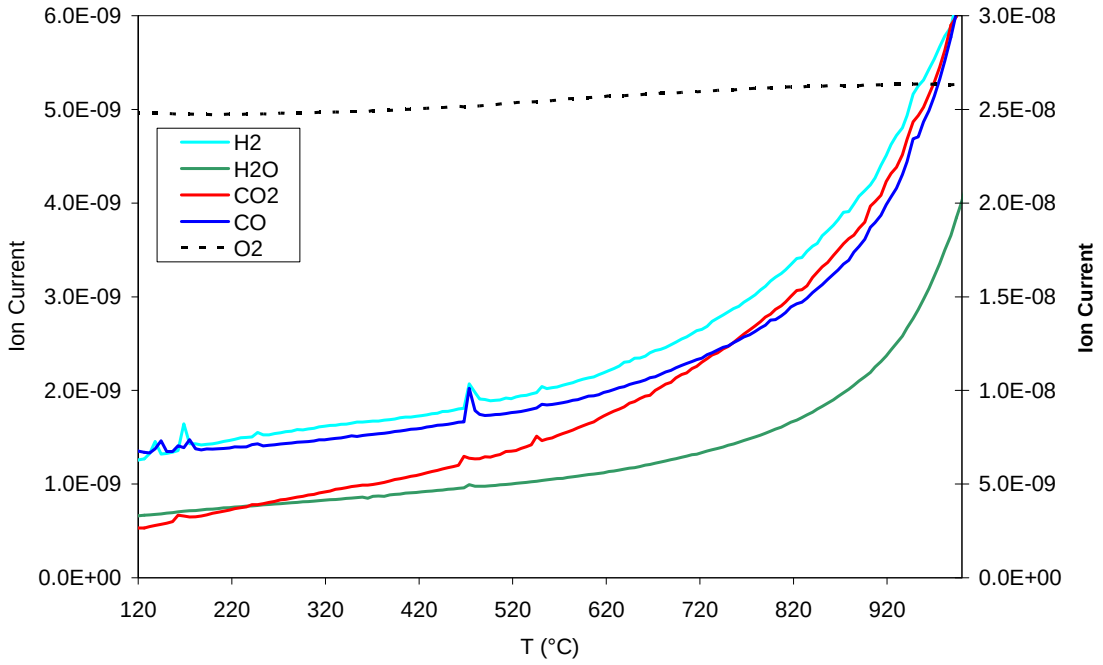

Figure 6.3. TPO Spectra of cleaved HOPG sample before ODH reaction, ($P(O_2)$: $1x10^{-7}$ mbar) *(right y axes corresponds to CO and O_2 signal)*

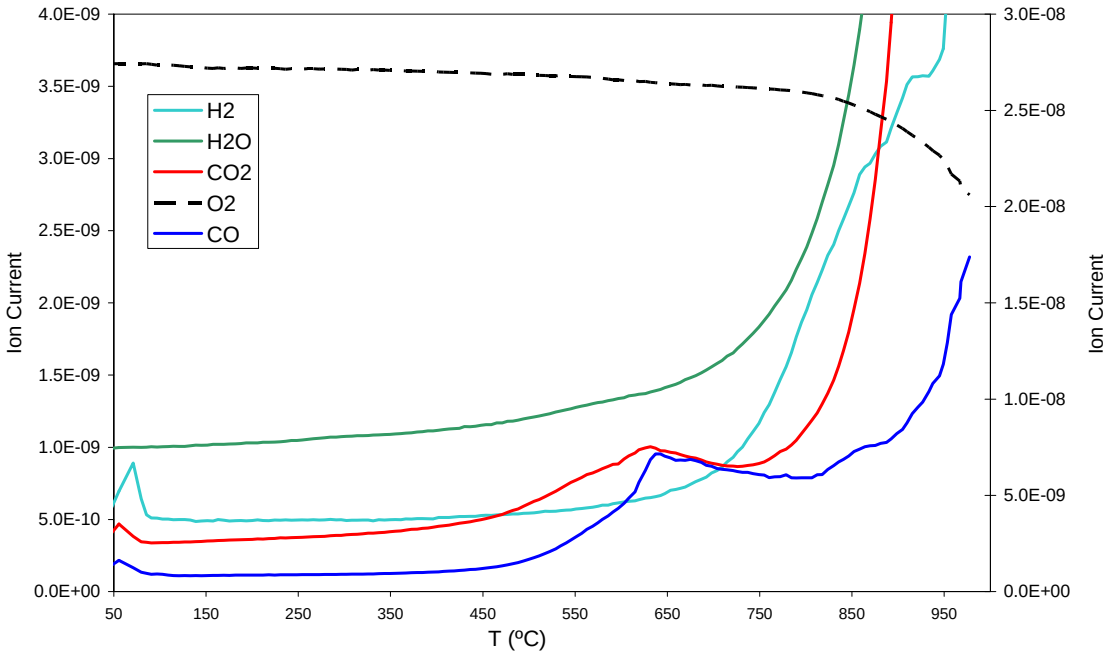

Figure 6.4. TPO ($P(O_2)$: $1x10^{-7}$ mbar) spectra of cleaved HOPG sample after ODH reaction. (20 ml/min, 0.5% EB, 1% O_2, 120 min, 400 ^{o}C)
(right y axes corresponds to CO and O_2 signals)

The oxidation/reduction properties of the carbon depositions were studied by performing thermal desorption experiment in a carbon monoxide atmosphere, such

an experiment can reveal information about the ability of these depositions to oxidize CO to CO_2, and hence the redox behaviour of these deposits. This in turn, gives more information about the nature of the available oxygen-containing groups since only aroxyl/phenol or quinine/hydroquinone groups can play a rule in redox processes[1-3].

Figure 6.5 shows the TP-CO spectra of a cleaved HOPG sample before reaction. The absence of any CO_2 production peak shows that this surface does not exhibit any red/ox activity at these conditions. The sharp peak at ~ 50 ^oC appearing here and elsewhere is caused by desorption from the heating filament which is situated behind the sample.

Figure 6.6 shows the desorption spectra of CO, CO_2, and H_2O in a TP(CO) experiment of an HOPG sample after ODH reaction of ethylbenzene (120 min, 400 ^oC). A peak of CO_2 appears at ~ 650 ^oC, which is the same peak observed by TPD and TPO. In addition to the fact that this peak was observed in the previous experiments in absence of CO, it is clear that this CO_2 peak is not a result of CO oxidation catalyzed by the surface depositions since it is not accompanied by any visible decrease in CO signal.

No visible change in the CO signal was observed at any temperature, except a peak at about 670 ^oC which is the same CO peak observed in TPD and TPO experiments. The sharp peak which appears at about 870 ^oC caused by an instantaneous fluctuation in heating filament current which is accompanied by the jump in CO and H_2 signals (degassing products). It, therefore, does not have any scientific importance.

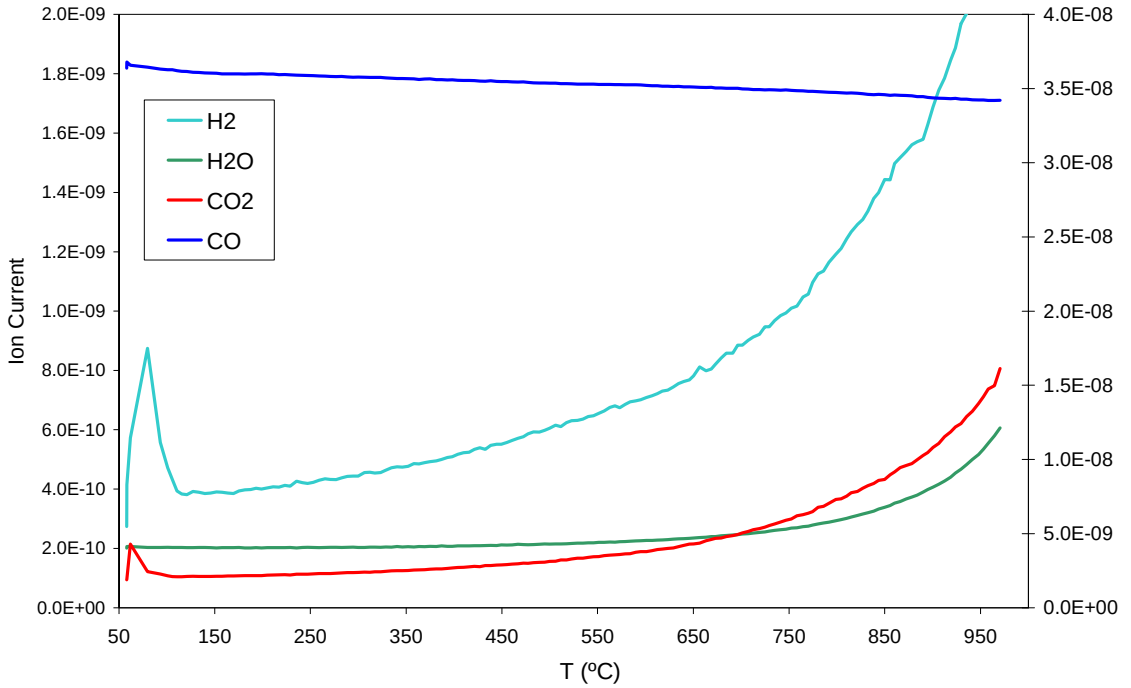

Figure 6.5. TP-CO spectra (P(CO): $1x10^{-7}$ mbar) of cleaved HOPG sample before ODH reaction *(right y axes corresponds to CO signal)*

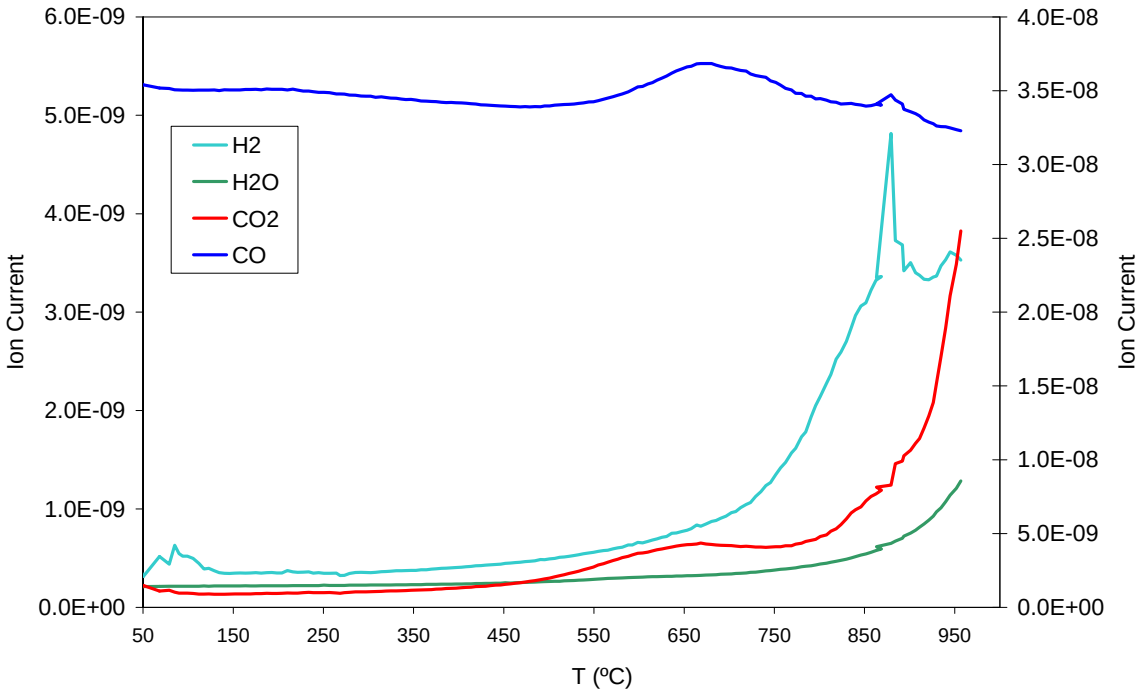

Figure 6.6. TP-CO spectra (P(CO): $1x10^{-7}$ mbar) of cleaved HOPG sample after ODH reaction (20 ml/min, 0.5% EB, 1% O_2, 120 min, 400 ^{o}C) *(right y axes corresponds to CO signal)*

6.2 Post reaction scanning electron microscope (SEM) images

To have a closer look on the surface of HOPG after reaction, SEM technique was used. Figure 6.7 shows the SEM images obtained of an oxygen-sputtered HOPG sample (30 min, 1keV, 1.5 μA) after reaction (shown in figure 5.11). SEM images were obtained at different beam energies which influences the depth sensitivity of SEM. Difference of depth sensitivity was utilized in producing better (depth understanding) of the observed surface features.

In figure 6.7, which is performed using electron beam energy of 5.0 keV, pits of different sizes can be seen on the surface, these pits can be seen clearly upon decreasing the electron acceleration voltage in figures 6.8, 6.9 and 6.10 obtained using 1.5, 0.7 and 0.5 kV acceleration voltage respectively.

Knowing that decreasing the electron beam energy increases the surface sensitivity of the electron beam, it can be concluded that the seen pits are located on the upper surface layers of the sample. The depth of these pits is supposed to be in the range of few atomic layers.

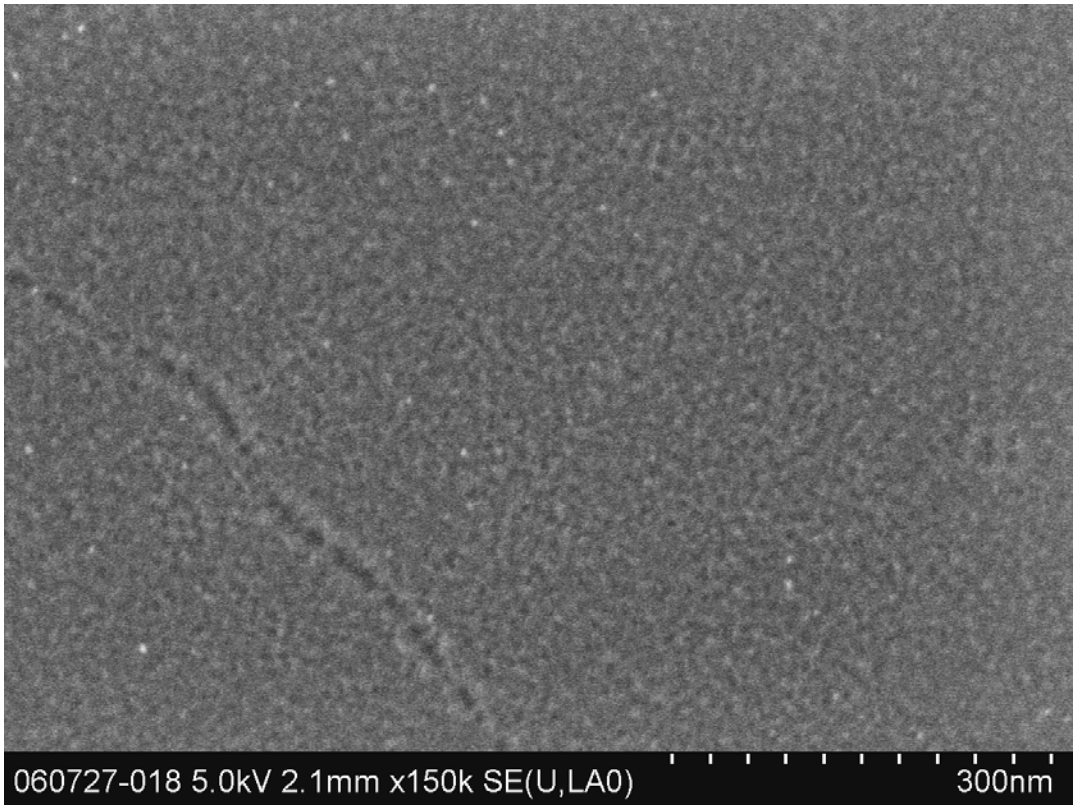

Figure 6.7. SEM image of oxygen-sputtered HOPG sample after ODH reaction.

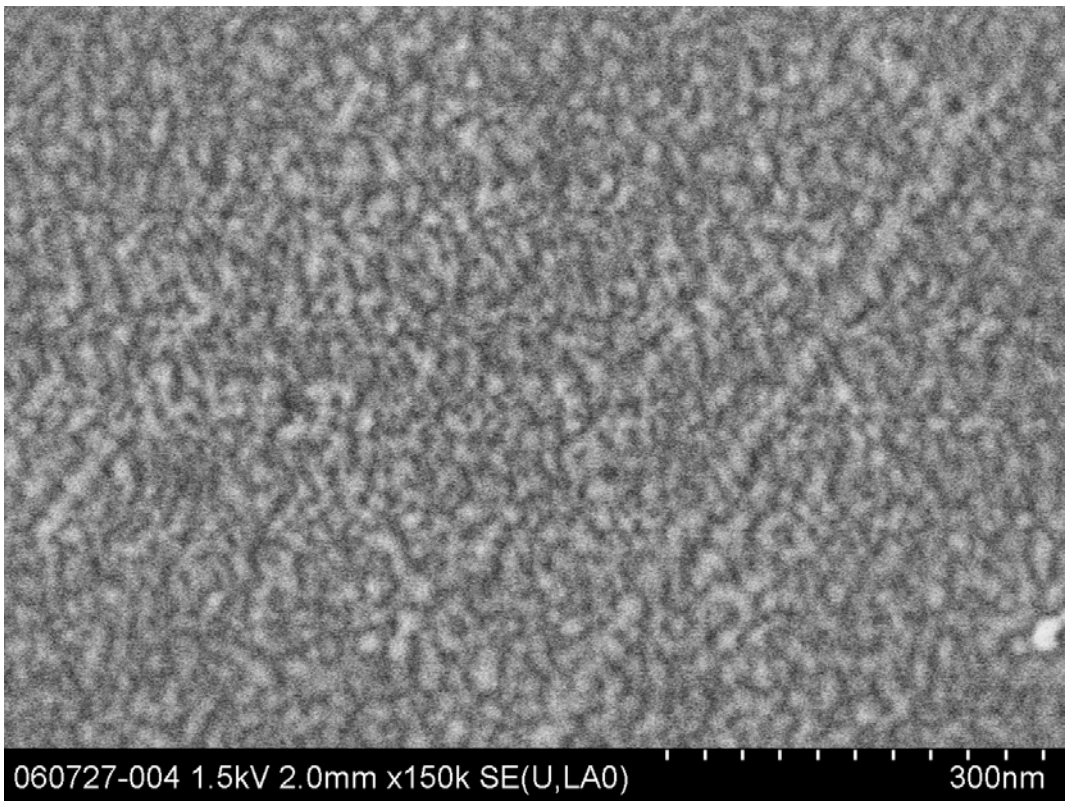

Figure 6.8. SEM image of oxygen-sputtered HOPG sample after ODH reaction.

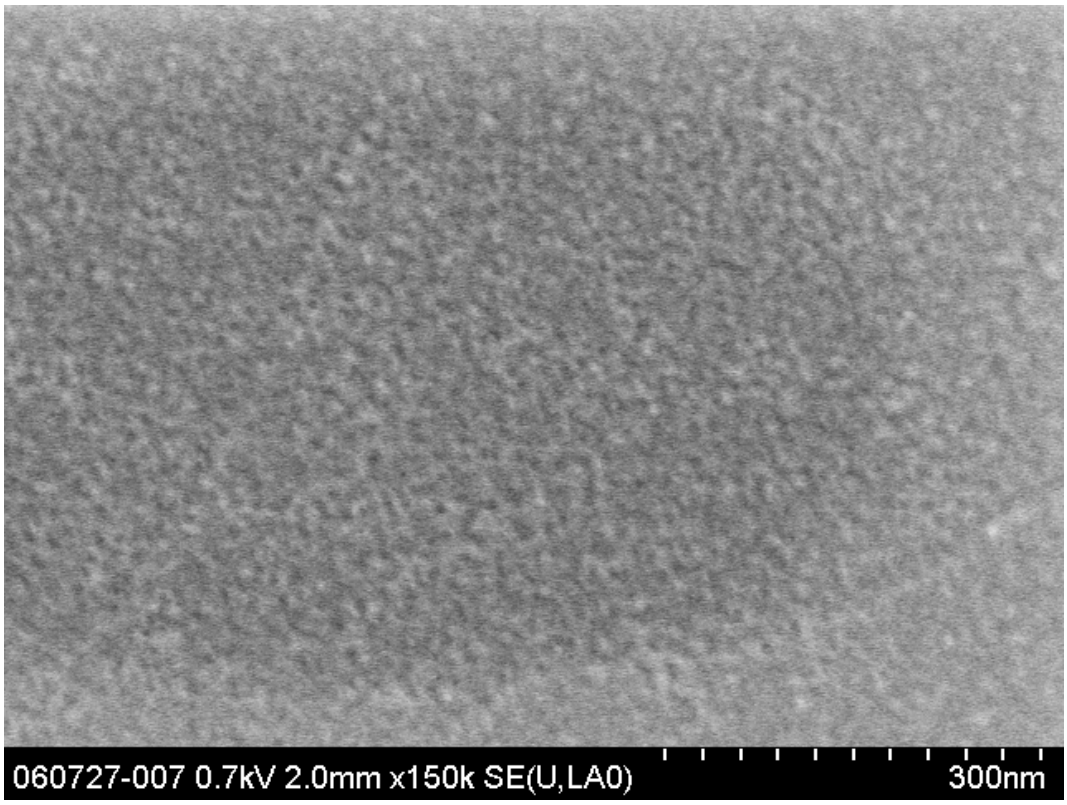

Figure 6.9. SEM image of oxygen-sputtered HOPG sample after ODH reaction.

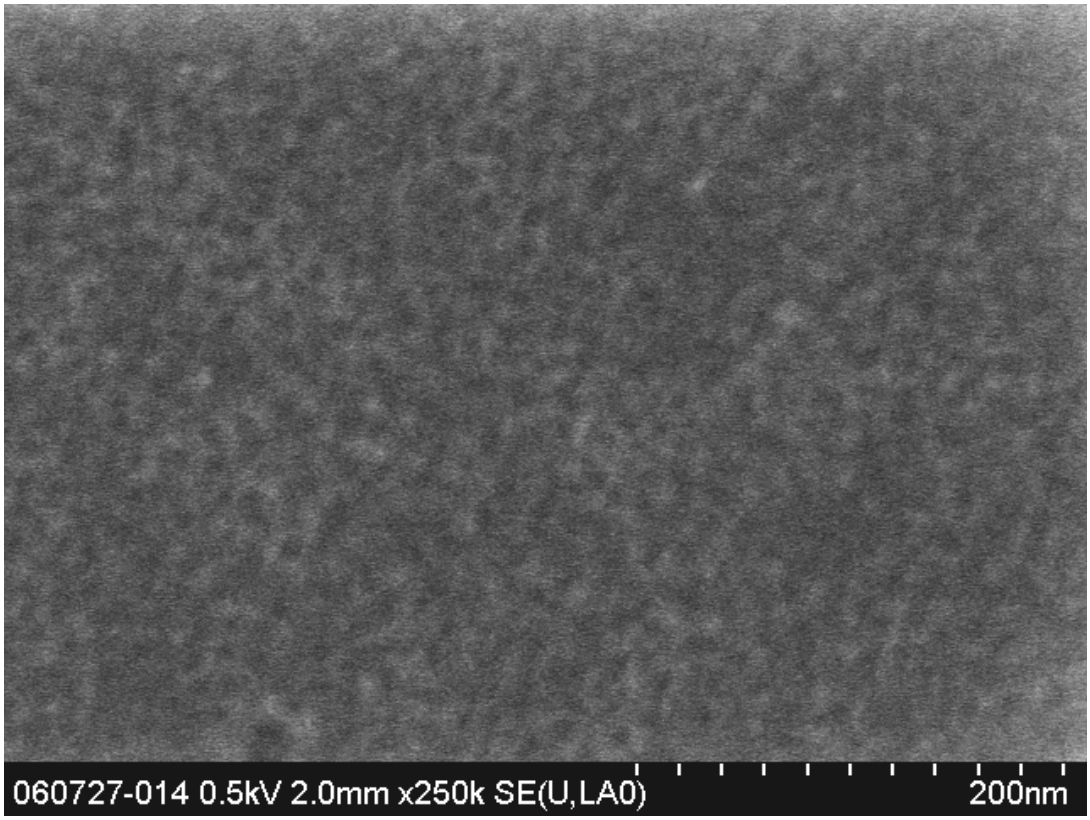

Figure 6.10. SEM image of oxygen-sputtered HOPG sample after ODH reaction.

6.3 Post reaction atomic force microscope (AFM) images

Additionally and to achieve better understanding of the reaction influence on the surface morphology, Atomic Force Microscopy (AFM) was used. AFM images were obtained for freshly cleaved HOPG, oxygen-sputtered HOPG, freshly cleaved reacted HOPG and oxygen-sputtered reacted HOPG samples.

Figure 6.11 shows an AFM image of a cleaved HOPG sample. The surface is clearly smooth and no features can be seen on the surface, just as expected for such a surface. The cleaved surface after reaction (300 min, 400-480 ^{o}C, 20 ml/min, 2:1 O2/Eb) which is shown in figure 6.12 looks smooth as well and comparable to the cleaved surface. This can be understood as the building of a uniform layer of graphitic carbon deposits on the smooth graphite surface resulting in a smooth surface as well, this is in agreement with the observations of Lisovskii et. al. in their study dealing with ODH of alkyl-benzenes over carbonaceous materials[4]. They stated

that “the carbonaceous materials is a system of condensed aromatic rings with conjugated double bonds”

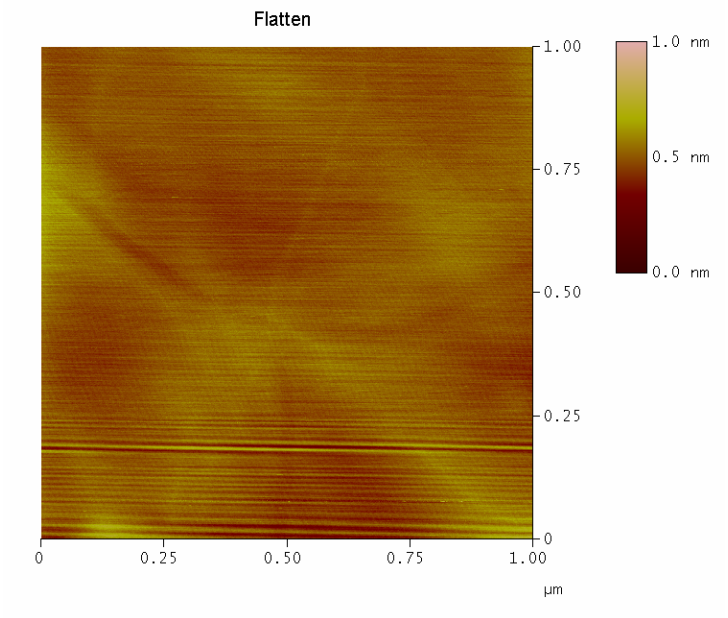

Figure 6.11. AFM image of cleaved HOPG

The AFM image of a oxygen-sputtered surface (5 min., 1 µA, 1 keV) is shown in figure 6.13. As expected, the surface is not smooth any more. The depth of surface pits is in the range of 1-3 monolayers.

Figure 6.14 shows the AFM image of the sputtered surface (30 min., 1 µA, 1 keV) after reaction (300 min, 400-480 ^{o}C, 20 ml/min, 2:1 O2/Eb). Interestingly, this surface was found to be the roughest surface. The observed roughness can be better seen in the shown section analysis, the pits depth in this case is up to 10 monolayers. It is obvious that the long sputtering of the sample played a significant rule in generating this roughness, it can be also seen that the reaction and the building of carbon deposits (which should be of graphitic nature as mentioned before) did not cover the whole surface causing a decrease in its roughness.

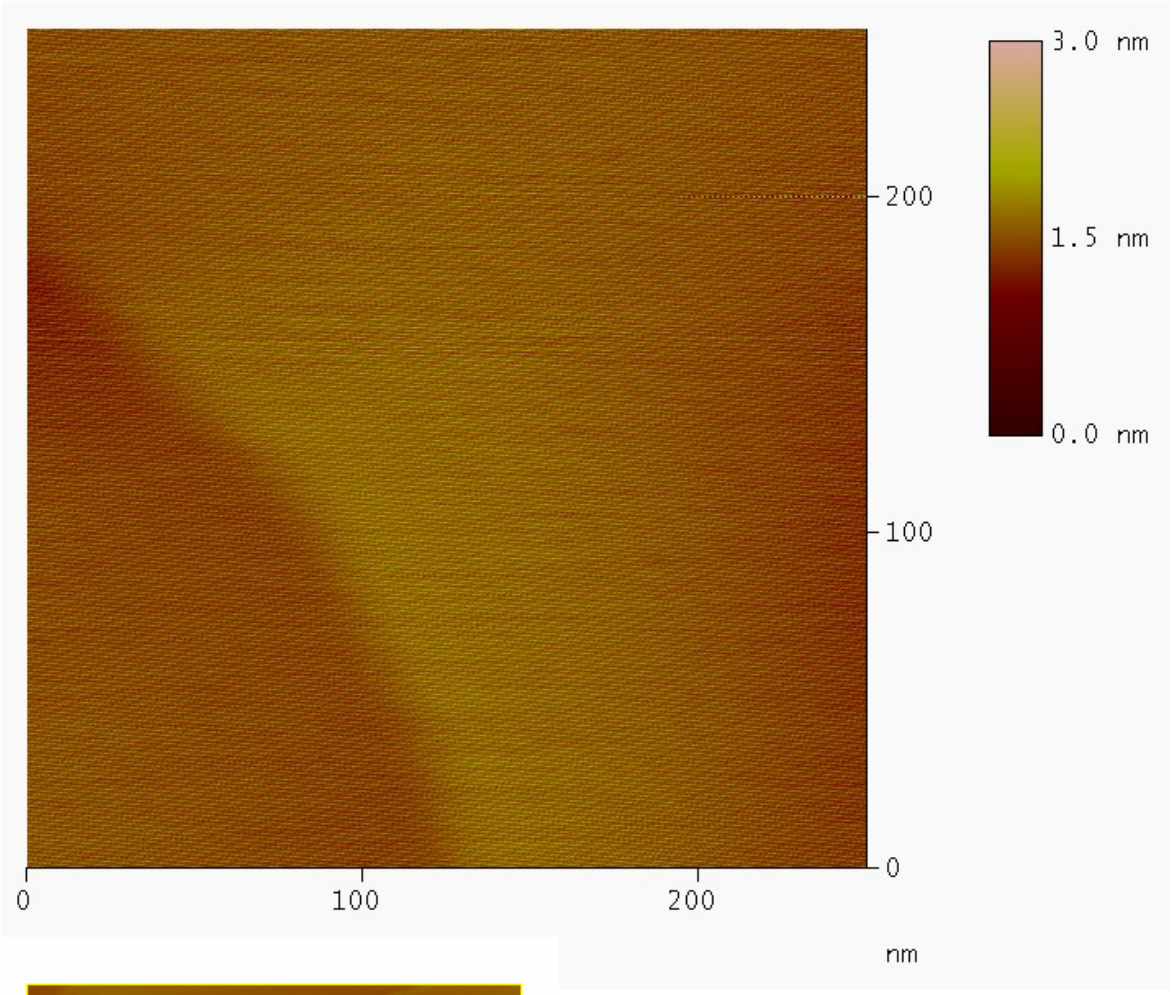

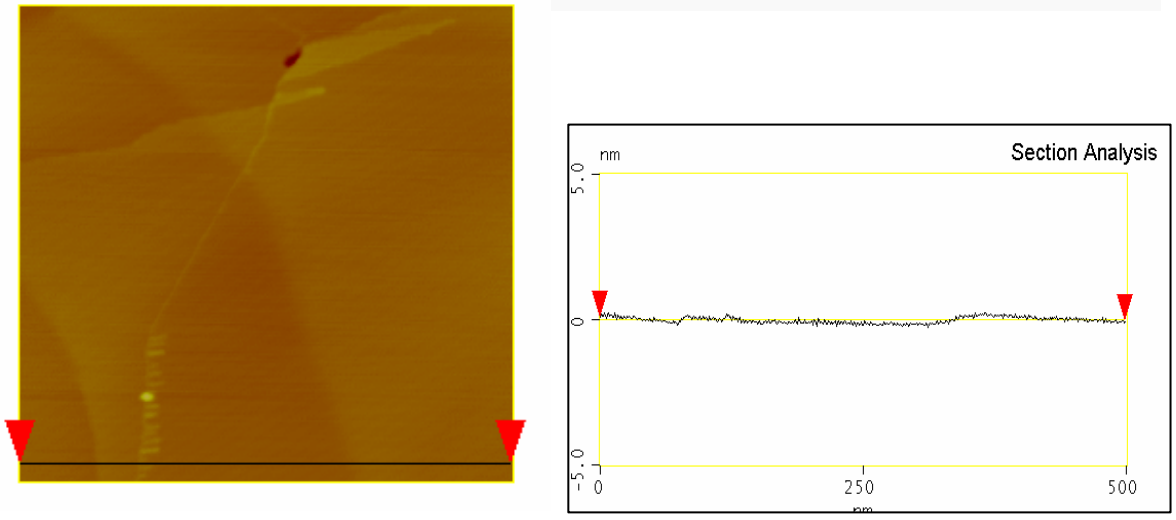

6.12. AFM image of cleaved HOPG after reaction.

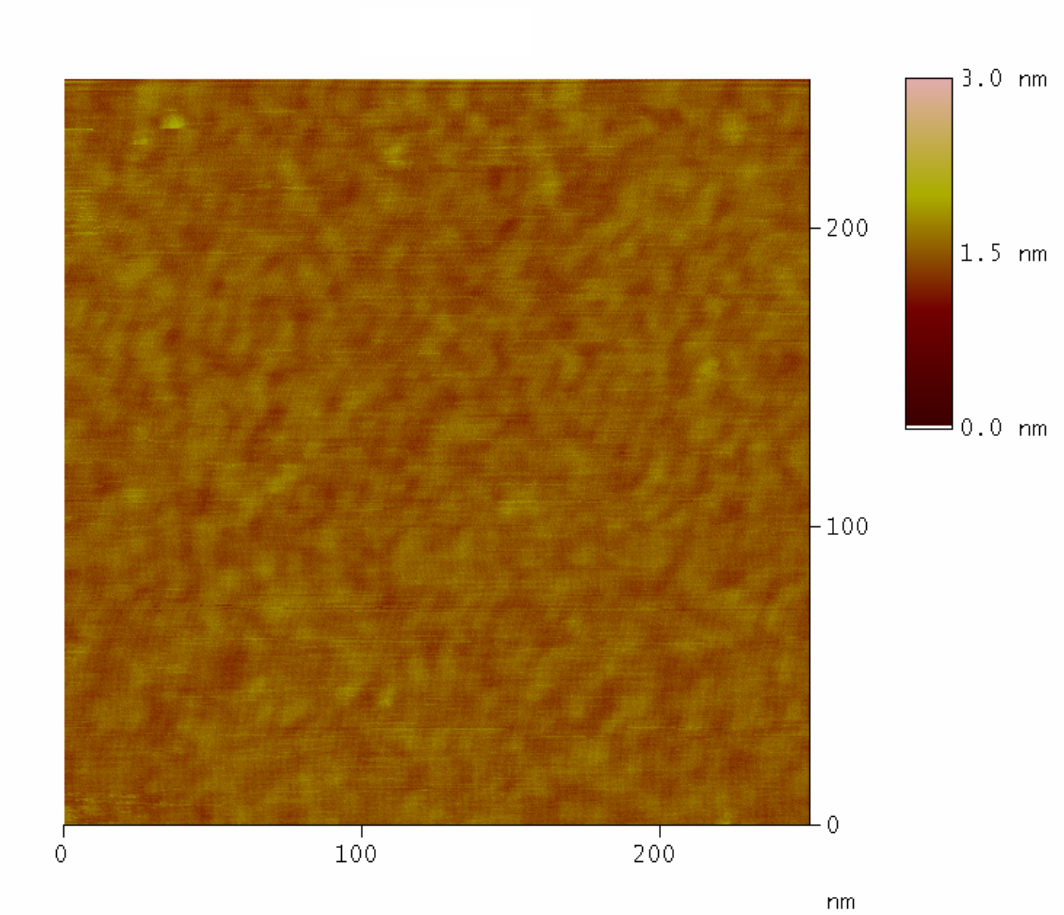

Figure 6.13. AFM image of oxygen-sputtered HOPG

Possible reason for this high roughness after reaction is the gasification of the destroyed (highly sputtered) regions of the HOPG surface by the action of oxygen at reaction conditions.

It is also possible that the reaction takes place only on some specific spots of the surface (ODH active centres), the reaction -as known- causes the building up of carbon depositions (which has its own catalytic activity, as well), these depositions in this case will build up on the top of the (active centres) blocking them and continue building up as hills increasing the surface roughness, this scheme is shown in figure 6.15.

As mentioned above, the carbon deposits are composed of condensed aromatic rings, this implies the graphitic character of these deposits, but does not mean that these deposits are simply graphite. Nevertheless, these deposits have significant

content of oxygen and can contain hydrogen in some cases depending on the reaction conditions and the nature of the catalyst.

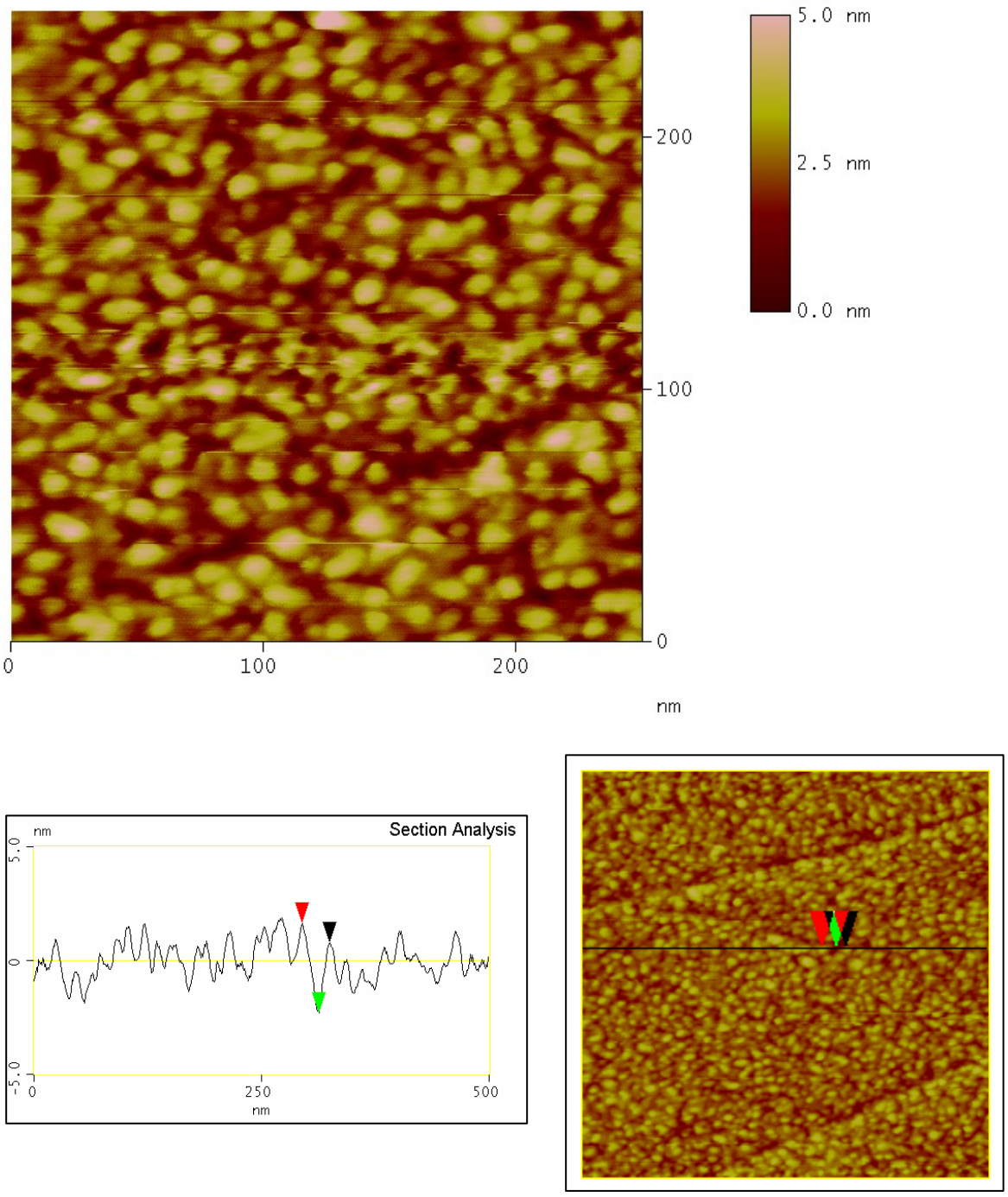

Figure 6.14 AFM image of oxygen sputtered HOPG after reaction.

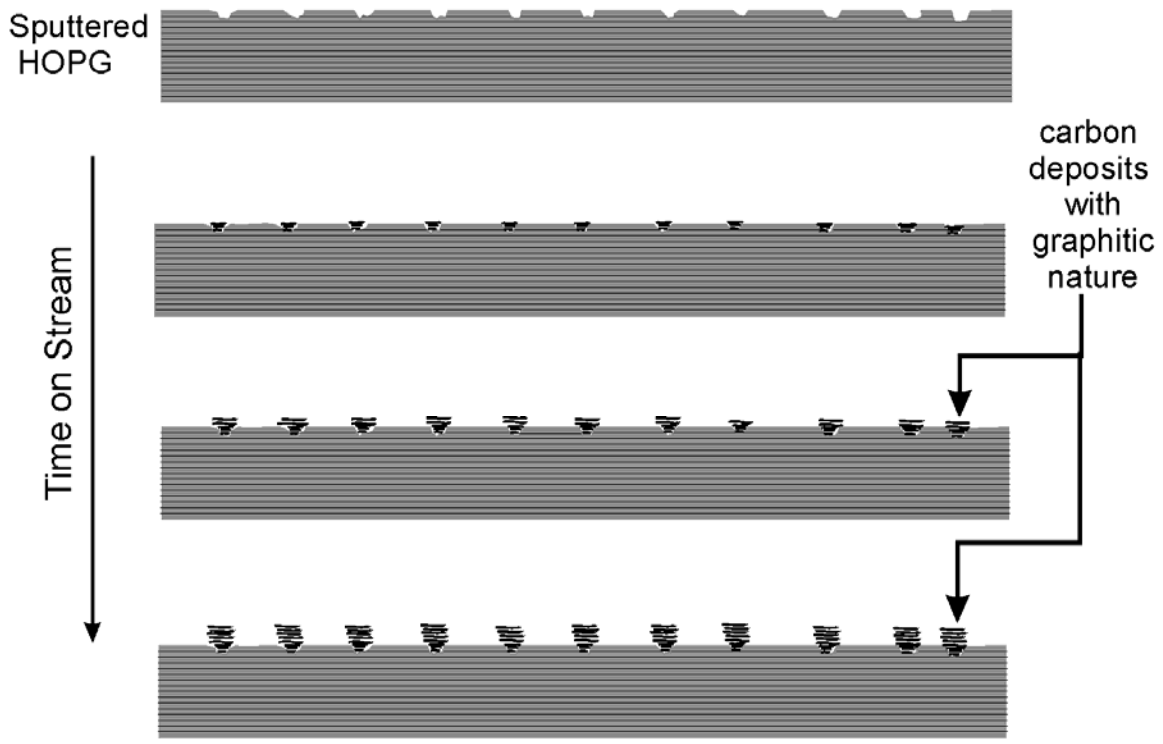

Figure 6.15 Scheme of building of carbon deposits over the active centers on the surface of HOPG during ODH reaction.

(1) Schraut, A.; Emig, G.; Sockel, H. G. *Applied Catalysis* **1987**, *29*, 311-326.
(2) D.S.Su , N. M., J.J.Delgado, N.Keller, G.Mestl, M.J.Ledoux, R.Schlogl *Catalysis Today* **2005**, *102–103*, 110 –114.
(3) Murakami, Y.; Iwayama, K.; Uchida, H.; Hattori, T.; Tagawa, T. *Journal of Catalysis* **1981**, *71*, 257-269.
(4) Lisovskii, A. E.; Aharoni, C. *Catalysis Reviews* **1994**, *36*, 25-74.